Optimal Scheduling of a Hydrogen-Based Energy Hub Considering a Stochastic Multi-Attribute Decision-Making Approach

Imeni, Mahyar Lasemi ; Ghazizadeh, Mohammad Sadegh ; Lasemi, Mohammad Ali; Yang, Zhenyu

Published in:
Energies

DOI (link to publication from Publisher):
10.3390/en16020631

Publication date:
2023

Document Version
Publisher's PDF, also known as Version of record

energies

MDPI

Article

Optimal Scheduling of a Hydrogen-Based Energy Hub Considering a Stochastic Multi-Attribute Decision-Making Approach

Mahyar Lasemi Imeni [1], Mohammad Sadegh Ghazizadeh [1], Mohammad Ali Lasemi [2] and Zhenyu Yang [2,*]

[1] Department of Electrical Engineering, Shahid Beheshti University, Tehran P.O. Box 19839-63113, Iran
[2] AAU Energy, Aalborg University, 6700 Esbjerg, Denmark
* Correspondence: yang@energy.aau.dk

Abstract: Nowadays, the integration of multi-energy carriers is one of the most critical matters in smart energy systems with the aim of meeting sustainable energy development indicators. Hydrogen is referred to as one of the main energy carriers in the future energy industry, but its integration into the energy system faces different open challenges which have not yet been comprehensively studied. In this paper, a novel day-ahead scheduling is presented to reach the optimal operation of a hydrogen-based energy hub, based on a stochastic multi-attribute decision-making approach. In this way, the energy hub model is first developed by providing a detailed model of Power-to-Hydrogen (P2H) facilities. Then, a new multi-objective problem is given by considering the prosumer's role in the proposed energy hub model as well as the integrated demand response program (IDRP). The proposed model introduces a comprehensive approach from the analysis of the historical data to the final decision-making with the aim of minimizing the system operation cost and carbon emission. Moreover, to deal with system uncertainty, the scenario-based method is applied to model the renewable energy resources fluctuation. The proposed problem is defined as mixed-integer non-linear programming (MINLP), and to solve this problem, a simple augmented e-constrained (SAUGMECON) method is employed. Finally, the simulation of the proposed model is performed on a case study and the obtained results show the effectiveness and benefits of the proposed scheme.

Keywords: smart energy hub; multi-energy carrier; renewable energies; uncertainty analysis; power-to-hydrogen; multi-criteria decision

Citation: Imeni, M.L.; Ghazizadeh, M.S.; Lasemi, M.A.; Yang, Z. Optimal Scheduling of a Hydrogen-Based Energy Hub Considering a Stochastic Multi-Attribute Decision-Making Approach. *Energies* **2023**, *16*, 631. https://doi.org/10.3390/en16020631

Academic Editors: Mohamed Benbouzid, Sinisa Durovic, Xiandong Ma and Hao Chen

Received: 1 December 2022
Revised: 22 December 2022
Accepted: 29 December 2022
Published: 5 January 2023

1. Introduction

1.1. Motivation

The integration of different energy systems consisting of multi-energy carriers is introduced as a sustainable solution to decrease the operational cost and reach decarbonization goals. In fact, this integration means coupling the different energy infrastructures together and making them possible to convert each energy carrier into another [1]. In this context, the energy hub concept has been proposed and developed by researchers with the aim of obtaining more efficient energy management for such an integrated energy system. Hydrogen is an emission-free energy carrier that can be used in the transport sectors as a green fuel. Since environmental pollution has become a major concern and carbon is the main component of greenhouse gases (GHG), the integration of hydrogen into energy systems can contribute to decarbonization. Moreover, using renewable energies to produce hydrogen while reducing emissions, can reduce operation costs in the whole energy system. Following the increment of pollutant emissions, in the near future, a large number of customers will lead to the use of renewable energy sources (RESs) [2]. Therefore, the investigation of integrated energy systems based on hydrogen and renewable energy resource would be one of the most important topics for the future of energy transition. For this purpose, considering the uncertainty of renewable energies as well as proposing an

accurate model of hydrogen-based equipment is an important point to bring the studies closer to reality.

1.2. Literature Review

According to the energy hub definition in the literature, it is considered a place that can receive different forms of energy carriers as input and supply different forms of energy demand as output. In recent years, diverse works have been done regarding the operation and optimization of energy hubs. These works can be distinguished from proposing different structures and models for energy hubs and utilizing different optimization models for their energy management. By developing different energy conversion technologies, such as combined heat and power (CHP), combined cooling, heat and power (CCHP), as well as energy storage system (ESS), the basis of different energy carrier integration has been formed [3]. On the other hand, hydrogen is considered a clean energy carrier and it is promoted to achieve a green energy system. Based on this fact, Power-to-Hydrogen (P2H) technologies has also been presented as a new concept in which electrical energy is converted to hydrogen. These technologies can play the role of ESS for energy buffering aims by using hydrogen tanks. Moreover, P2H can participate in ancillary services for electrical networks because electrolyzers have a fast response [4]. To deal with the low efficiency of electrolyzers, a new power-to-hydrogen and heat (P2HH) system has been introduced by Li et al. [5]. Liu et al. [6] proposed a novel method considering P2H and power to methane (P2M) with the aim of maximizing wind power participation and minimizing the total operation cost. Jahangir et al. [7] used a hydrogen/diesel backup system in the energy hub to improve operation cost by considering discount and inflation rates. Shabani et al. [8] presented a new model by assuming agents for all facilities that participate in the cooperative model to maximize their own profit and social welfare.

Shaving loads, especially during peak periods, has a significant impact on the operation cost and can even affect the emission cost. DRP is one of the most important tools for modifying the loads with respect to energy prices. Majidi et al. [9] presented a new smart energy hub model to support electrical and thermal demand by using DRP for decreasing the total operation cost. Integrated demand response programming (IDRP) for both electrical and thermal demand has been introduced by Jamalzadeh et al. [10] for the energy hub system, connected to electrical, natural gas, and district heating networks. Saatloo et al. [11] have proposed a novel robust optimization approach in which the system operational cost was reduced by approximately 7.8%, considering electricity price uncertainty as well as IDRP for electrical and heating loads. Another important issue in the operation of energy hubs is uncertainty analysis. A data-driven approach based on regression techniques is applied to estimate the renewable energies from historical data in [12]. To handle wind uncertainty, Daneshvar et al. [13] presented scenario-based stochastic optimization by using Monte Carlo simulation to generate different scenarios for modeling wind fluctuation. Turi et al. [14] reviewed and analyzed the potential of wind energy in Pakistan and showed that using RESs has a significant effect on reducing the GHG emissions emitted from the energy sectors in Pakistan. Javadi et al. [15] applied photovoltaic as a renewable energy resource (RES) of the energy hub and proposed a novel model to operate the energy hub by considering a scenario-based method for the PV generation and energy demand uncertainty.

A bilevel optimization model has been also used by Bostan et al. [16] for day-ahead optimal scheduling of energy hub and the advantage of the proposed method has been demonstrated by testing it on the IEEE 33 bus standard system as a case study system. The simulation results have shown the proposed method reduces distribution system costs by approximately 27.8%. Risk-based optimal scheduling for an energy hub system has been presented by Karkhaneh et al. [17] to avoid encountering abnormally high costs in the possible scenarios determined by the system operator. A novel stochastic model for hydrogen- and water-based energy hub has been given by Kafaei et al. [2] with the aim of minimizing the operation cost and carbon emission. To analyze the system's random

variables, a hybrid uncertainty method was employed in the proposed problem. The scenario-based method has been considered for modeling electric vehicle uncertainty and information gap decision theory (IGDT) has been used for modeling the uncertainty of the renewable resource. Multiple integrated energy hubs with industrial consumers are presented in [18] to minimize its operation cost, considering a competitive energy market environment. The uncertainty of the day-ahead electricity market price, energy demand, and PV generation have been considered in the proposed model. Tao et al. [19] proposed a new model for the IES including electrical, gas, and hydrogen energy carriers, aiming to supply electrical and hydrogen loads without considering RESs uncertainty. The results have shown that this integration of multi-energy carriers can increase social welfare and decrease total operation costs. A novel hydrogen-based energy hub has been given by AlRafea et al. [20] to increase the renewable energy sources penetration considering combined cycle power plants through electrolysis generating hydrogen. The obtained results showed a 2% reduction in total energy cost. It should be noted that in this reference, DRP was not studied. Optimal planning for an electricity-hydrogen system considering N-1 contingency and robust optimization to address PV, wind turbine, and load uncertainty has also been presented by [21]. In Table 1, the details of the recent studies are shown, and the superiority of the proposed method will be proved.

Table 1. Detail of recent studies on energy hub.

Ref	CM	EM	MOO	DM	EDRP	TDRP	EESS	HESS	WT Uncertainty	PV Uncertainty
[9]	✓	×	×	×	✓	×	✓	×	×	✓
[10]	✓	×	×	×	✓	✓	✓	×	×	×
[13]	✓	×	×	×	✓	✓	✓	×	✓	✓
[15]	✓	×	×	×	×	×	✓	×	×	✓
[16]	✓	×	×	×	✓	×	✓	×	✓	✓
[17]	✓	✓	×	×	✓	✓	×	✓	✓	✓
[2]	✓	✓	×	×	×	×	✓	✓	✓	✓
[18]	✓	×	×	×	✓	✓	✓	✓	×	✓
[22]	✓	×	×	×	✓	✓	✓	✓	✓	×
[21]	✓	×	×	×	×	×	✓	✓	✓	✓
[7]	✓	✓	×	×	×	×	✓	✓	×	×
[23]	✓	✓	✓	×	✓	×	✓	×	×	✓
[24]	✓	✓	✓	×	✓	×	✓	×	×	×
[25]	✓	✓	✓	×	×	✓	×	✓	✓	×
[26]	✓	✓	✓	✓	×	✓	×	×	✓	×
Proposed paper	✓	✓	✓	✓	✓	✓	✓	✓	✓	✓

In Table 1 symbol ✓ and × mean the subject is considered and not considered in related studies. According to this table, there are different studies in which some of the aforementioned subjects are taken into consideration, but there is no research that has a comprehensive study on all subjects. For example, in [10,17,25], uncertainty of WT and PV is not considered. Moreover, IDRP has only been considered in [10,13,17,18,22], and none of the other references have used this tool. Another important point in this paper is considering hydrogen as the primary energy in the energy system. Although some references have considered P2H facilities in their research, none of them have considered hydrogen as the base energy. Additionally, the problems in all references except [18–20] are single objectives and only ref. [20] uses DM for achieving the best answer among Pareto optimal solutions. In this study, SAUGMECON, which is more powerful than other e-constraint methods, is used to generate optimal Pareto solutions and AHP is used as the DM method.

1.3. Contribution

In this paper, a novel stochastic energy hub scheduling is given, considering detailed modeling for hydrogen network and IDRP. The proposed problem is introduced as a multi-objective optimization problem in the frame of mixed-integer non-linear programming (MINLP). The first one is the minimization of the energy hub operation cost and the second one is the minimization of the greenhouse gas emission. Moreover, this paper gives a comprehensive and coherent approach from historical data analysis as input of the proposed problem to final decision-making as its output. This approach can be divided into 3 sections, i.e., uncertainty handling, optimization, and decision-making. A scenario-based approach is first employed to model the uncertainty of wind and solar, with regard to uncertainty handling. Then, the simple augmented e-constrained (SAUGMECON) is implemented to obtain Pareto front optimal solutions for the optimization part. Finally, a new procedure is applied to reach the best possible solution by using analytic hierarchy process and weighted sum methods based on the pay-off table. The contributions of this paper can be summarized as follows:

- Proposing detailed modeling of hydrogen-based equipment to achieve a more realistic operation of an energy hub;
- Proposing an IDRP containing EDRP and TDRP to reduce both operation and emission costs;
- Wind and solar generation uncertainty modeling by applying a scenario-based method;
- Presenting a novel multi-objective optimization problem for optimal operation of the energy hub by employing SAUGMECON to reach Pareto optimal solution;
- Using the AHP method as a multi-criteria decision-making procedure to select the desired solution.

1.4. Organization

This paper is organized as follows: energy hub modeling is presented in Section 2. Problem formulation and all equations about the model are given in Section 3. Then, the solution methodology is discussed in Section 4. First, SAUGMECON as a multi-objective optimization method and then AHP as multi-criteria decision-making are described in this section. In the next section, the case study and the simulation results are comprehensively discussed. Finally, Section 6 is dedicated to the conclusion of the paper.

2. Proposed Energy Hub

In each energy hub, some forms of energies are considered as inputs of energy hub and some as outputs. Based on that, the relation between the energy hub's inputs and outputs can be presented as Equation (1) [27].

$$[P_{out}] = [C][P_{in}] \tag{1}$$

where C is a converter coupling matrix, P_{in}, and P_{out} are inputs and outputs vectors, respectively. Figure 1 presents the proposed energy hub in this paper. As shown in this figure, the proposed energy hub includes hydrogen, electricity, and natural gas as input energy carriers and supplies hydrogen, electrical, gas, and heat demand. The proposed energy hub has different own facilities to maintain energy demand besides selling these energies through upstream energy networks. For instance, to supply electrical demand, the electricity can be provided by the direct generation of the solar and wind turbine and or through fuel cells by converting hydrogen to electricity. In the proposed energy hub, hydrogen demand is also considered and is met by electrolyzer and hydrogen network. Moreover, EESS and HESS are considered for energy price market balancing through saving electricity and hydrogen when the price is low and use it when the electrical and hydrogen network price is high.

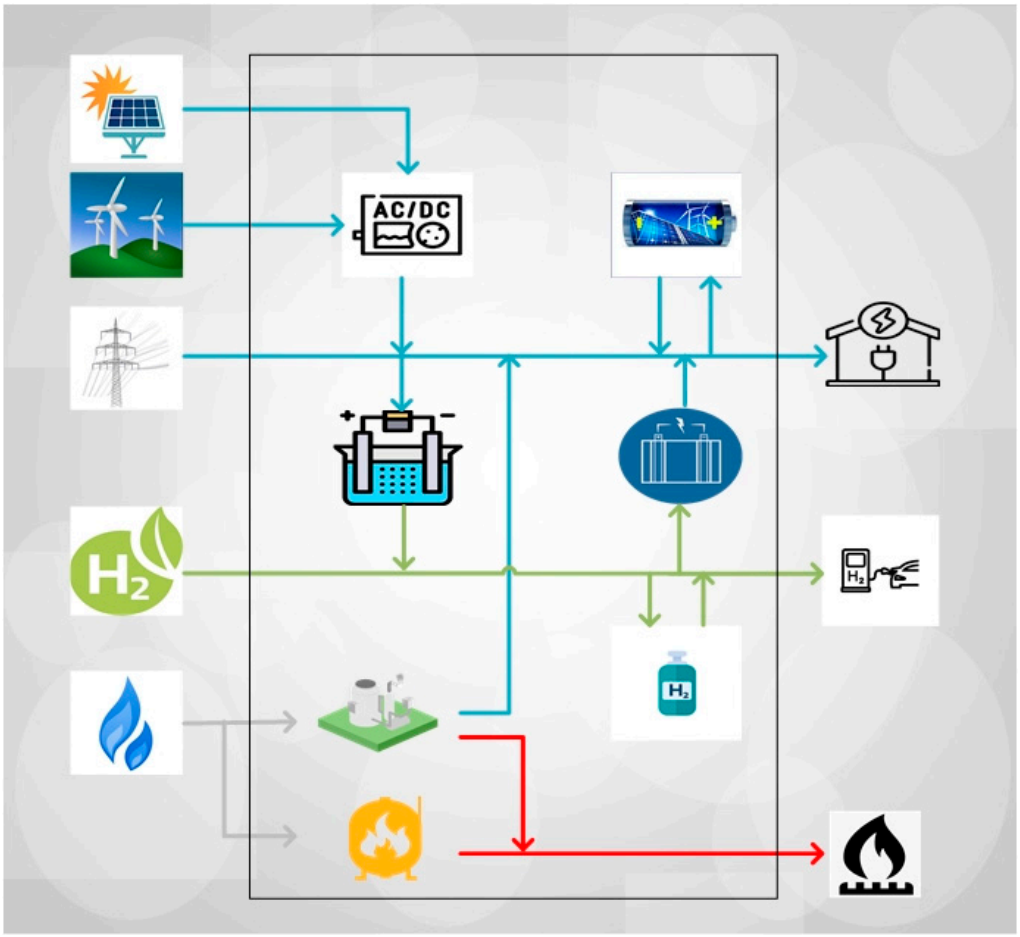

Figure 1. Proposed energy hub architecture in this study.

3. Problem Formulation

3.1. Objective Function

The proposed problem is given as two-objective optimization problem. The first objective is to minimize the total operation cost of the energy hub, which is presented by Equation (2). This cost function consists of the cost of the electricity, natural gas, and hydrogen purchased from the upstream grids, as well as EESS, TESS, EDRP and TDRP operation costs. In the second objective function, given by Equation (3), the amount of emission produced by the energy hub and energy networks is minimized. The emission function includes two main parts. The first part is the distribution of greenhouse gases during the operation of energy hub equipment, such as CHP and boiler. This part is called the energy hub inside emissions. The second part deals with the distribution of greenhouse gases during the generation and transportation of energy in the energy networks, which is related to the energy carriers consumed by the energy hub. This part is called the energy hub outside emissions. The proposed problem objective functions are as follows:

$$Z_1 = Min\left\{\sum_{t=1}^{24} \lambda_e(t).P_e(t) + \lambda_g(t).P_g(t) + \lambda_{H_2}(t).P_{H_2}(t) + \lambda_{H_2}^{ST}\left[P_{H_2}^{ch}(t) + P_{H_2}^{dis}(t)\right] + \lambda_e^{ST}\left[P_e^{ch}(t) + P_e^{dis}(t)\right] + \sum_{cr\in\{e,h\}} \lambda_{cr}^{DR}(t)[L_{inccr}(t) + DR_{cr}(t).D_{cr}(t)]\right\} \quad (2)$$

$$Z_2 = Min\left\{\sum_{t=1}^{24} \gamma_{CHP}P_g^{CHP}(t) + \gamma_B P_g^B(t) + \gamma_g P_g(t) + \gamma_e P_e(t)\right\} \quad (3)$$

3.2. System Modeling

As an important point to achieve balance in any energy system, production and consumption must be always equal. For this reason, electrical, gas, heat and hydrogen energy balance are considered in the proposed energy hub. The energy balance constraints for electrical, gas, heat and hydrogen are presented in Equations (4)–(7), respectively. In these equations, input powers appear with positive sign and output powers appear with negative sign.

$$D_e(t) = \eta^T P_e(t) + \eta^C (P_{wT}(t) + P_{PV}(t)) - P_{EL}(t) + P_{FC}(t) + \eta_e^{CHP} P_g^{CHP}(t) - P_e^{ch}(t) + P_e^{dis}(t) \quad (4)$$

$$P_g(t) = P_g^{CHP}(t) + P_g^B(t) \quad (5)$$

$$D_h(t) = \eta^B P_g^B(t) + \eta_h^{CHP} P_g^{CHP}(t) \quad (6)$$

$$D_{H_2}(t) = P_{H_2}(t) + \eta^{EL} P_{EL}(t) - P_{FC}(t) - P_{H_2}^{ch}(t) + P_{H_2}^{dis}(t) \quad (7)$$

The system storage units are modeled by Equations (8) and (10) and restrictions (9) and (11). Equations (8) and (10) show that the amount of electrical and hydrogen power stored in EES and HES in $t = 1,\ 24$ must be equal to the initial values. Restrictions (9) and (11) are limitation of electrical and hydrogen power stored in storages.

$$P_{e\ storage}(t) = P_{e\ storage}(initial) \qquad \forall t = 1,\ 24 \quad (8)$$

$$P_{e\ storage}^{min} \times I_e(t) \le P_{e\ storage}(t) \le P_{e\ storage}^{max} \times I_e(t) \quad (9)$$

$$P_{H_2\ storage}(t) = P_{H_2\ storage}(initial) \qquad \forall t = 1,\ 24 \quad (10)$$

$$P_{H_2\ storage}^{min} \times I_{H_2}(t) \le P_{H_2\ storage}(t) \le P_{H_2\ storage}^{max} \times I_{H_2}(t) \quad (11)$$

In hydrogen-based equipment, an electrolyzer is used for converting electricity to hydrogen when hydrogen price is high. This electrical energy can be supplied from the power grid and wind turbine. Exactly opposite of electrolyzer, fuel cell convert hydrogen to electrical power when electricity price is so high. Restrictions (12) and (13) represent fuel cell and electrolyzer input power limit, respectively. Restriction (14) demonstrates that electrolyzer and fuel cell cannot operate at the same time.

$$P_{FC}^{min} \times I_{FC}(t) \le P_{FC}(t) \le P_{FC}^{max} \times I_{FC}(t) \quad (12)$$

$$P_{EL}^{min} \times I_{EL}(t) \le P_{EL}(t) \le P_{EL}^{max} \times I_{EL}(t) \quad (13)$$

$$I_{FC}(t) + I_{EL}(t) \le 1 \quad (14)$$

Restrictions (15)–(17) show electricity, gas, and hydrogen network constraints, respectively. CHP is used to convert natural gas into heat and electrical energy and also, boiler convert natural gas into heat energy which their allowable ranges presented by restrictions (18) and (19), respectively.

$$P_e^{min} \le P_e(t) \le P_e^{max} \quad (15)$$

$$P_g^{min} \le P_g(t) \le P_g^{max} \quad (16)$$

$$P_{H_2}^{min} \le P_{H_2}(t) \le P_{H_2}^{max} \quad (17)$$

$$0 \le P_g^{CHP}(t) \le P_g^{CHP\ max} \quad (18)$$

$$0 \le P_g^B(t) \le P_g^{B\ max} \quad (19)$$

Respectively, Equations (20) and (21) define the molar flows of electrolyzer and fuel cell. HESS pressure is obtained by Equation (22). Restriction (24) shows the limitation of HESS pressure which cannot exceed its maximum and minimum allowable limit. Considering

Faraday's low, molar flow of charging HESS (electrolyzer) and molar flow of discharging HESS (fuel cell) can be written as fallows [28]:

$$N_{EL}(t) = \frac{\eta^{\mathrm{EL}} P_{H_2}^{ch}(t)}{LHV_{H_2}} \tag{20}$$

$$N_{FC}(t) = \frac{P_{H_2}^{dis}(t)}{\eta^{\mathrm{FC}} LHV_{H_2}} \tag{21}$$

$$Pr_{H_2}(t) = Pr_{H_2}(t-1) + \frac{\Re T_{H_2}}{V_{H_2}}(N_{EL}(t) - N_{FC}(t)) \tag{22}$$

$$Pr_{H_2}(t) = Pr_{H_2}(initial) \qquad \forall t = 1 \tag{23}$$

$$Pr_{H_2}^{min} \leq Pr_{H_2}(t) \leq Pr_{H_2}^{max} \tag{24}$$

Equation (25) presents the relation between wind speed and WT output power [29]. According to this formula, if wind speed be between v_r and v_{co}, WT generate its maximum output power. Furthermore, (26) shows the electrical power generated from PV system [30].

$$P_{WT}(t) = \begin{cases} 0 & v(t) \leq v_{ci} \text{ or } v(t) \geq v_{co} \\ P_r . \frac{v(t) - v_{ci}}{v_r - v_{ci}} & v_{ci} \leq v(t) \leq v_r \\ P_r & otherwise \end{cases} \tag{25}$$

$$P_{PV}(t) = \frac{Irr(t)}{Irr_0} \times \left\{ P_{max}^{M} + \mu_{max} \times \left[T(t) + Irr(t) \times \frac{NOCT - 20}{800} - T_0 \right] \right\} \tag{26}$$

3.3. Demand Response

DRPs are used to achieve lower operation costs, by shifting the load from on-peak hours to off-peak hours. DRPs are programs that encourage consumers to reduce their energy consumption by changing the consumption pattern of consumers according to the price of energy during the day. It is noted that DRP just effected on operation cost and there is no effect on greenhouse gas emission. There are many programs to use, but in this paper TOU demand response programming is used.

$$D(t) - Load(t) = DR(t)D(t) - L_{inc}(t) \tag{27}$$

$$DR(t) \leq DR^{max}(t) \tag{28}$$

$$\sum_t L_{inc}(t) = \sum_t DR(t)D(t) \tag{29}$$

4. Solution Methodology

In this paper, a comprehensive methodology is presented to find the final solution of the proposed problem. In this way one of the strongest methods, i.e., SAUGMECON, is firstly used to figure out Pareto optimal solution and after a multi-criteria decision-making method is employed to reach the best solution among all candidate solutions on the Pareto front. In the rest of this section, the solution methodology employed in this research is described in detailed.

4.1. Multi-Objective Optimization Method

To solve the multi-objective problem and reach a reliable solution, it is necessary to employ a multi-objective Pareto-based method. In this paper, SAUGMECON method is presented to solve the propose problem and generate Pareto optimal solutions. This method is a combination of traditional and augmented e-constrained method [31]. In this method, one objective considered as a main objective function and the other objectives are assumed

as inequality constraints. Then, pay-off tables components are obtained by solving the single objective problem for each constraint and after that, Pareto optimal solutions will be reachable. Consider an original optimization problem as follows:

$$Min\ \{Z_1(X), Z_2(X),\ \ldots,\ Z_n(X)\} S.\ to: \qquad h(X) = 0 g(X) \leq 0 X \in S \tag{30}$$

The objective function consists of Z_1, Z_2, $\ldots$, Z_n that constrained to some equality and some inequality constraints and S is the feasible solution. By using the SAUGMECON method, the proposed multi-objective problem transformed as follows:

$$\begin{array}{c} Min \left\{ Z_1(X) - eps \times \frac{Z_2(X)}{r_2} + \frac{Z_3(X)}{r_3} + \ldots + \frac{Z_n(X)}{r_n} \right\} \\ S.\ to: \qquad Z_2(X) \leq e_n^k \quad Z_3(X) \leq e_3^k,\ \ldots\ ,\ Z_n(X) \leq e_n^k \\ h(X) = 0 \\ g(X) \leq 0 \\ x \in S \end{array} \tag{31}$$

where (Chamandoust et al., 2019):

$$e_n^k = Z_n^{max} - \left(\frac{Z_n^{max} - Z_n^{min}}{q_n} \right) \times k \qquad k = 1,\ 2,\ \ldots\ ,\ q_n \tag{32}$$

In which eps is scaling factor ($10^{-6} \leq eps \leq 10^{-3}$), r_n and q_n are the range and number of equal intervals of nth objective function. The advantage of SAUGMECON method is that the main objective function is optimized completely, and the other objectives optimized as much as possible. Additionally, in this method inefficient Pareto optimal solutions are not produced. These make the augmented method answer faster than the traditional method.

4.2. Multi-Criteria Decision Making

In this step, after providing Pareto optimal solutions by the SAUGMECON, a decision maker should choose the most preferred solution among the Pareto optimal solutions based on the preferences of the decision making. In this study, AHP is used to determine the weighting factors of each objective function [32]. To implement this method, at first the pairwise comparison matrix should be created. For the proposed problem, this matrix will be as follows:

$$A = \begin{bmatrix} 1 & a_{12} & \ldots & a_{1p} \\ \frac{1}{a_{12}} & 1 & \ldots & a_{2p} \\ \vdots & \vdots & \ddots & \vdots \\ \frac{1}{a_{1p}} & \frac{1}{a_{2p}} & \ldots & 1 \end{bmatrix} \tag{33}$$

where a_{ij} is quantified judgment on a Z_i and Z_j that $a_{ij} = \frac{1}{a_{ji}}$. The pairwise comparison between the two criteria can be considered by applying the priority value from 1 to 9, according to the importance of each objective compared to the other objective.

After placing desired numbers in the matrix A, largest eigenvalue (λ_{max}) and its relevant normalized eigenvector (V) are calculated. Components of this normalized eigenvector are the same as the weighting values for all objective functions. In this paper, three decision making are considered and the value of each component in each step is presented in Table 1. At the last stage, before defining certain weighting values, consistency of the comparison matrix should be verified.

$$CR = \frac{CI}{RI} \tag{34}$$

$$CI = \frac{(\lambda_{max} - n)}{(n-1)} \tag{35}$$

RI values for different numbers of criteria are shown in Figure 2. If $CR \leq 0.1$, the obtained eigenvector as weighting values are acceptable [32]. After using the AHP method and obtaining the adequate weights, the main objective function would be calculated as follows:

$$Z = \omega_1 \times \frac{Z_1}{Z_1^{min}} + \omega_2 \times \frac{Z_2}{Z_2^{min}} \quad (36)$$

where Z_1^{min} and Z_2^{min} are provided in Table 2 according to Equation (36); if one of coefficients is zero, the objective function will be equal to 1.

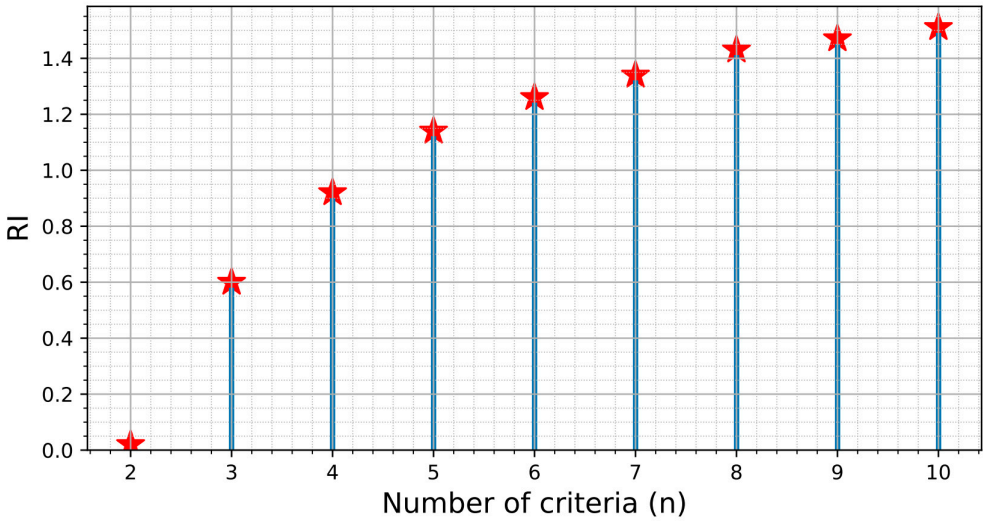

Figure 2. Relation between *RI* and *n* to qualify the comparison matrix.

Table 2. Pay-off table calculated for the proposed problem.

OF	Z_1	Z_2
***Min* Z_1**	194,906.3	11,776.401
***Min* Z_2**	243,094.586	10,058.488

5. Case Study

As mentioned earlier, the aim of this paper is to simultaneously minimize the operational cost and carbon emissions for local integrated energy systems in the presence of P2X technologies, considering the EH concept. To achieve this goal, the MINLP problem is implemented in Python with by using Pyomo package. The local energy system, considered as case study for this research, is connected to upstream energy systems including electricity, gas, and hydrogen networks. The energy price for these energy carriers is shown in Figure 3. As can be seen from this figure, the price of electricity is very variable, unlike the price of hydrogen. Figure 4 shows the hydrogen load profile for each time interval. All facilities and networks parameters are considered based on [25,33,34]. It is also assumed that the hydrogen produced in the hydrogen network is green hydrogen, so hydrogen production does not cause any pollution. However, the electricity and natural gas produced by electricity and gas networks through fossil fuels resources and EH operators should pay emission costs for buying them.

To avoid the high deviation of the cost function of the optimization problem, it is necessary to normalize the value of objective functions based on the weighted sum method according to Equation (36). For this purpose, a pay-off table is determined. To calculate the pay-off table values, solving two single objective function is needed, so that the elements of the first row for this table, regarding the amount of Z_1 and Z_2, are calculated, while the first objective function is minimized. In the same way to find the amount of the second row elements, the second objective function should be minimized [35]. A pay-off table for the proposed problem has been shown in Table 2.

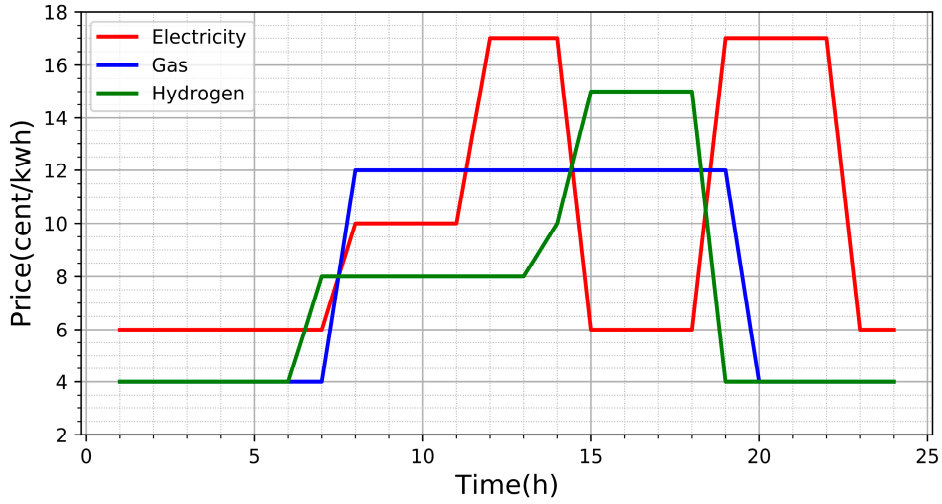

Figure 3. Electricity, gas and hydrogen price for the case study.

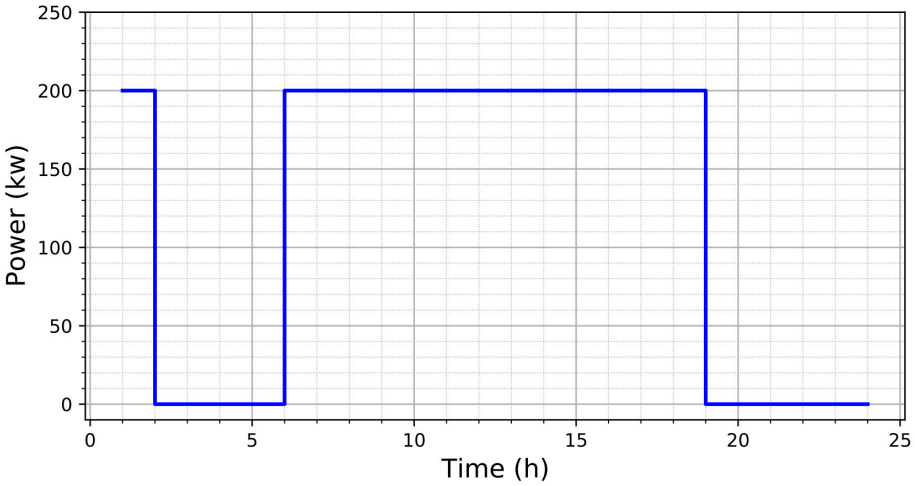

Figure 4. Hydrogen load profile of hydrogen demand.

After implementing SAUGMECON and obtaining optimal Pareto front solutions, according to AHP method, pairwise comparison matrices are calculated to achieve weight of objective functions. The elements of pairwise comparison matrices, largest eigenvalue, and most significant eigenvector of each case are shown in Table 3. As can be seen in this table, three case studies are assumed for the proposed problem in this paper according to reached weight factors for each objective function. These cases are as follows:

- Case-1: $\omega_1 = 0.8$ and $\omega_2 = 0.2$;
- Case-2: $\omega_1 = 0.5$ and $\omega_2 = 0.5$;
- Case-3: $\omega_1 = 0.2$ and $\omega_2 = 0.8$.

where ω_1 and ω_2 are coefficients of first and second objective functions, respectively.

Table 3. Obtained weights of each criteria from AHP method.

Decision Making	Criteria	Pairwise Comparison Matrix	Largest Eigenvalue	Largest Eigenvector
Case-1	Z_1 Z_2	$\begin{bmatrix} 1 & 4 \\ \frac{1}{4} & 1 \end{bmatrix}$	2	0.8 0.2
Case-2	Z_1 Z_2	$\begin{bmatrix} 1 & 1 \\ 1 & 1 \end{bmatrix}$	2	0.5 0.5
Case-3	Z_1 Z_2	$\begin{bmatrix} 1 & \frac{1}{4} \\ 4 & 1 \end{bmatrix}$	2	0.2 0.8

6. Simulation Results

As mentioned before, this paper presents a novel stochastic energy hub scheduling considering hydrogen network. To model the wind farm and PV uncertainty, 1000 scenarios are, respectively, generated by Python considering Weibull and Normal distribution. In the next step, the probability interval method is used for scenario reduction. In this procedure, the total distance of each scenario from the other scenarios is firstly calculated. A scenario, which has the shortest distance, is selected as an agent and all scenarios that their distance was less than the considered radius, are eliminated. Finally, five scenarios, shown in Figures 5 and 6, are chosen for the system simulation. The rest of this section gives the results obtained by solving the proposed problem. For better analyses, the simulation results are discussed in three sections.

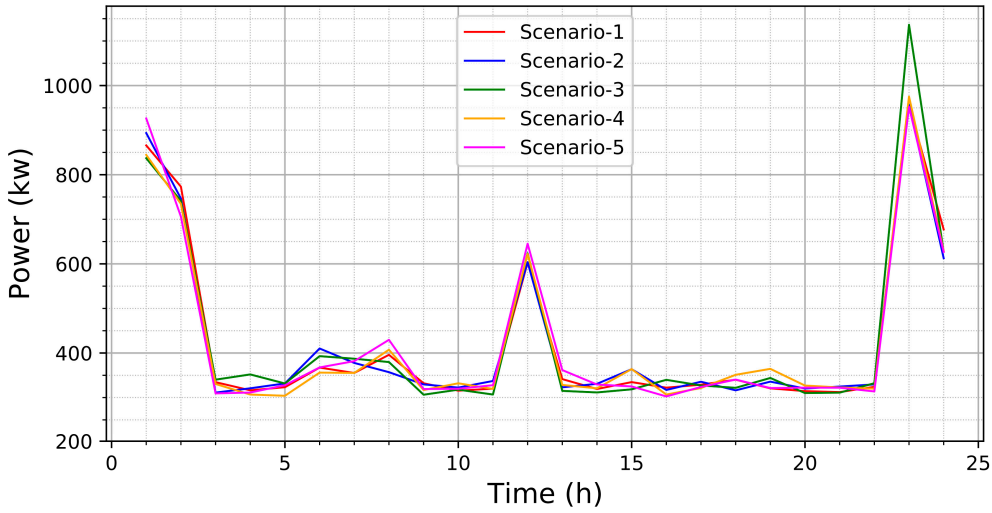

Figure 5. Wind farm generation for five scenarios selected by interval method.

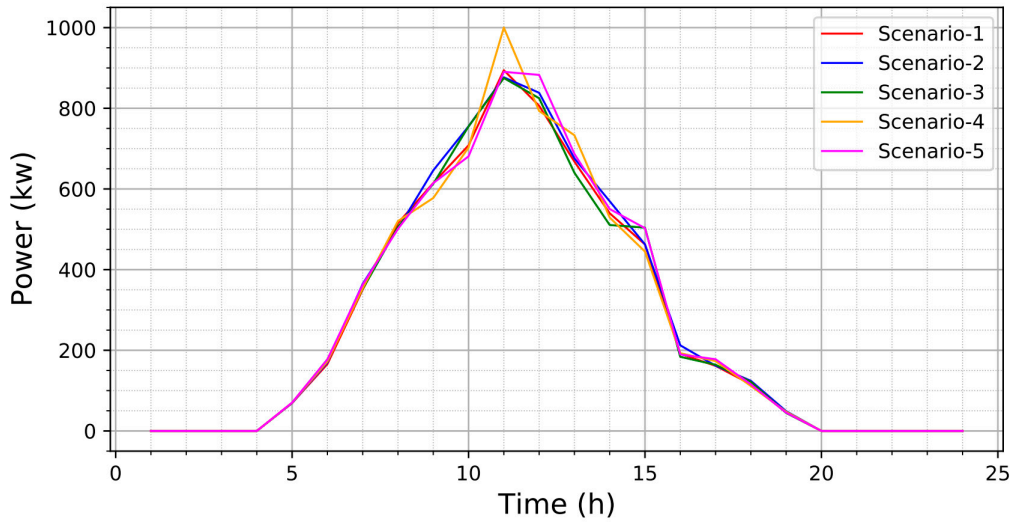

Figure 6. PV generation for five scenarios selected by interval method.

6.1. Energy Transaction with Upstream Networks

In this section, the results obtained in relation to the energy exchange between the energy hub and upstream energy networks are provided and discussed. To this end, the DRP effect is firstly investigated for each case in the operation results. Then, the energy exchange results are presented based on the load profile corrected by applying DRP. Figures 7 and 8 show the electricity and thermal demand before and after DRP, respectively. Considering the base load in Figure 7, there are three load levels for electricity demand

as follows; 1–8 and 24 are off-peak, 9–17 are mean-peak and 18–23 are on-peak hours. As can be seen from these figures, the implementation of DRP causes loads to be shifted from hours when the energy price is high to hours when the energy price is low or the contribution of renewable energy is high. For instance, for electricity loads, DRP shift loads from hours 12–14 and 19–22 to hours 24–6, and for heat loads, the loads are shifted from hours 8–19 to hours 20–23 and 3–6 to reduce operation cost. From the obtained results, it can be found that DRP has more effect on Case-1 than Case-2 as well as Case-2 than Case-3 because DRP is defined based on minimizing the operation cost, thus when the weight of Z_1 is reduced, the role of DRP is diminished as well.

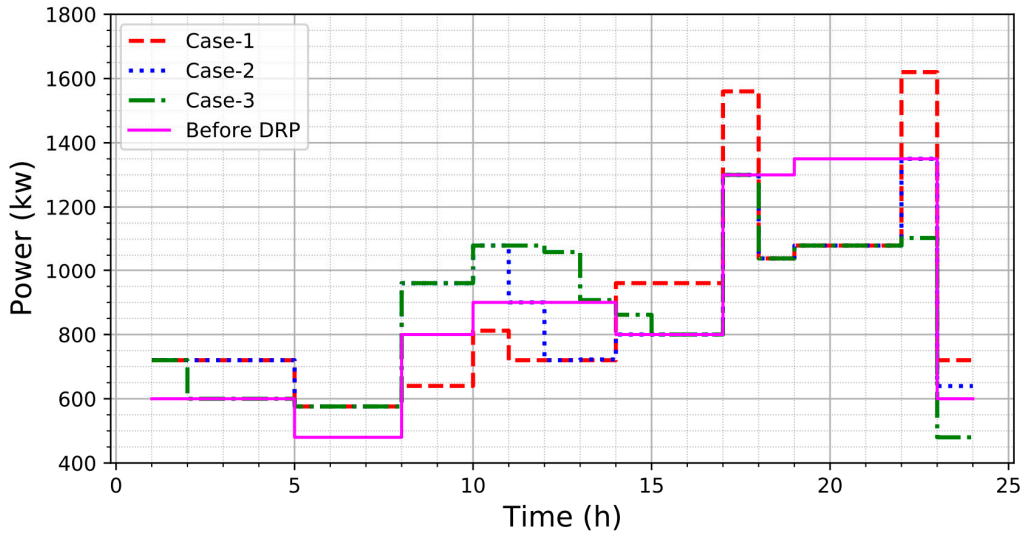

Figure 7. Electricity load profile before and after DRP for three cases.

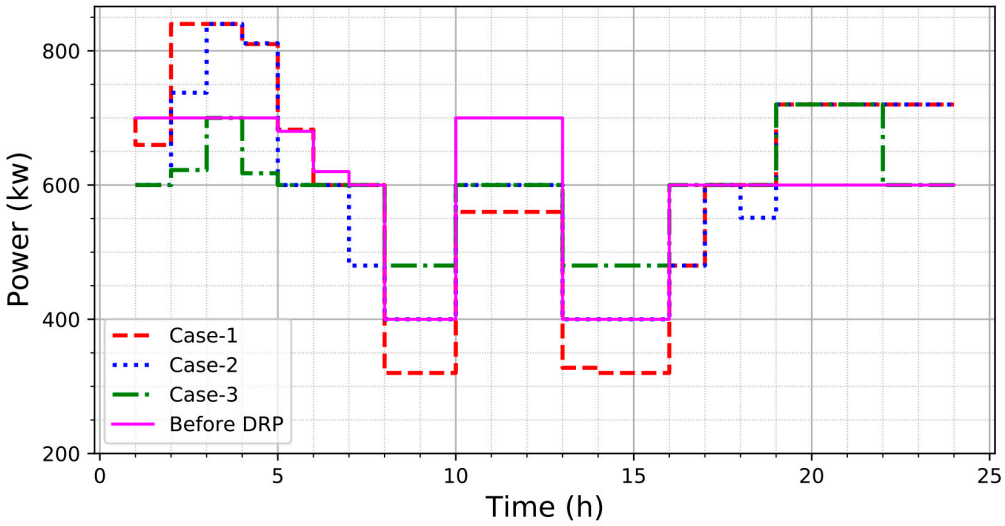

Figure 8. Thermal load profile before and after DRP for three cases.

Figure 9 shows the transaction of electrical energy between energy hub and upstream electrical network. In hours 7–14, when the generation power of WT and PV are at a sufficient level, the energy hub sells its excess power to the power grid with the aim of improving the objective function. The amount of the transacted electrical power in Case-3 is greater than other cases on hours 4–5 and 20–22, which are shown in Figure 9 with gold dashed boxes. In these hours, the fuel cell is operated on its maximum power; so, the energy hub must meet other demand using CHP or the electrical network. Since in Case-3 the emission cost is more important than the operational cost, as well as the electrical

network pollution being less than the gas network, the EH prefers to purchase its required electrical energy from the electrical network.

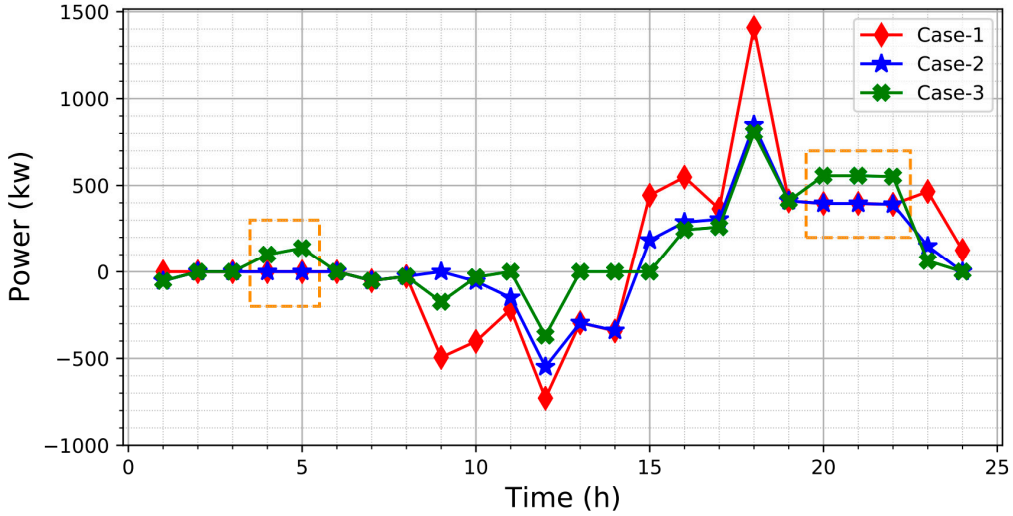

Figure 9. The electrical power exchange between energy hub and electrical network.

Figures 10 and 11 show the gas and hydrogen power purchased from natural gas and hydrogen upstream networks, respectively. According to Figure 10, the gas purchased from the gas network in Case-3 is more than in other cases at hours 9–10 and 14–17 because the thermal load of Case-3 after DRP is more than Case-1 and Case-2, as can be seen from Figure 8. In Case-3, the coefficient of emission cost is higher than the operation cost coefficient. In this situation, it is expected that cleaner energy carriers will be used more than others. As can be seen from Figure 11, the power purchased from the hydrogen network in Case-3 is more than in the other two cases during hours 9–18 and at hours 3, 5, and 20. Because the green hydrogen energy is clean and non-polluting the proposed EH uses more hydrogen in this case to Case-1 and Case-2, by considering the priority of the emission cost in Case-3.

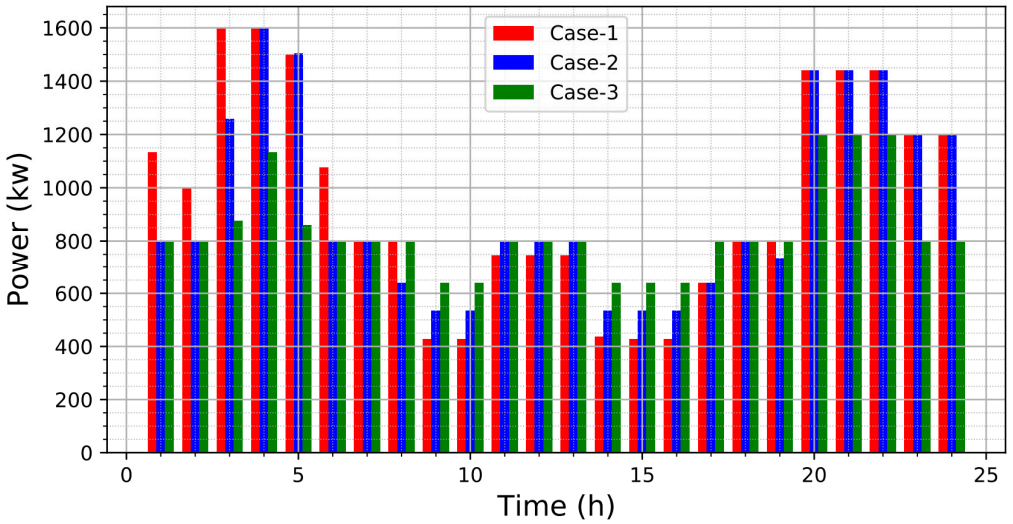

Figure 10. The gas power purchased from upstream network.

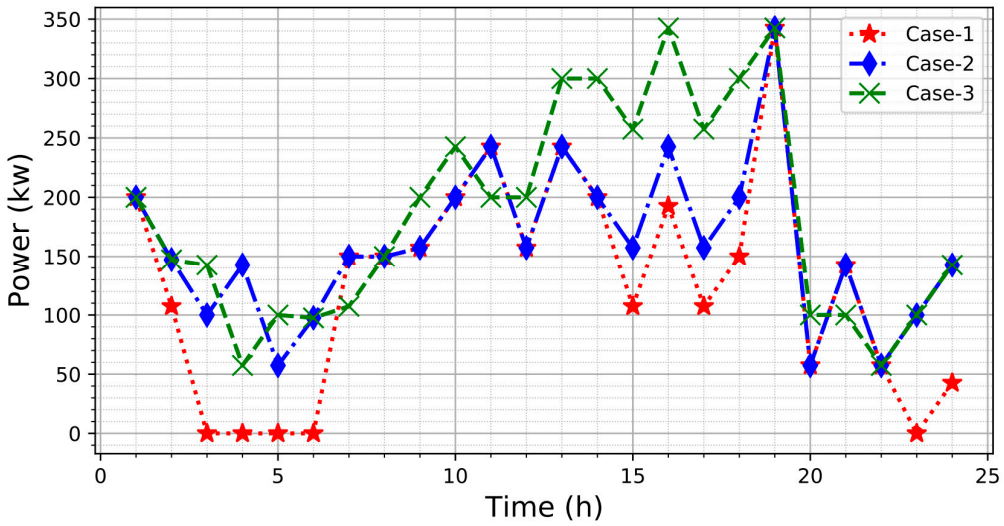

Figure 11. The hydrogen power purchased from upstream network.

6.2. Energy Exchange inside of the Energy Hub

In this section, the results regarding energy exchange inside of the energy hub are given. The amount of electrical energy stored in EESS and HESS are shown in Figure 12. As illustrated in this figure, the electrical energy stored in the EESS is used to meet the electrical demand during hours 3–7 and 19–23, when the WT and PV generation are reduced as shown in Figures 5 and 6. On the other hand, the energy storage systems are considered for energy price adjustment in different energy systems. This issue can also be seen in the results by comparing the results belonging to Case-1 in which the economic cost minimization is more important than emission minimization with the results of other cases. Based on the results obtained, the EESS is discharged at hours 9–10 and 14 to maximize the electrical power sold, with the aim of increasing the total system's benefit. As shown in Figure 12, the amount of power discharge is more for Case-1 than for other cases.

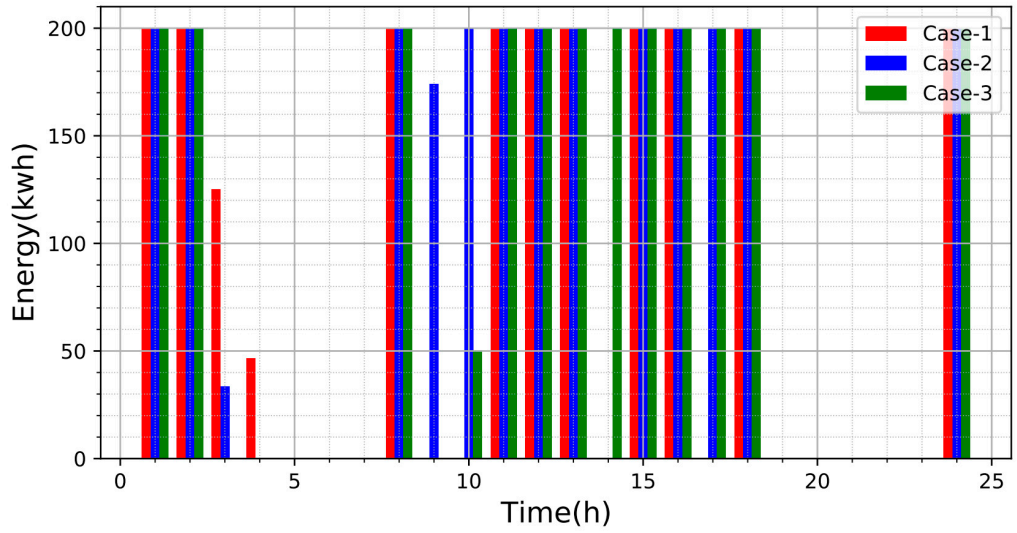

Figure 12. Electrical energy stored in EESS.

The amount of hydrogen energy stored in HESS as well as the internal pressure of HESS are, respectively, shown in Figures 13 and 14. By comparing these two figures, it is visible that HESS pressure has direct relation with the energy stored in HESS as described by Equations (20)–(24). Moreover, as mentioned earlier, green hydrogen is stored more for future usage in Case-3 than in the other cases, due to its non-pollution characteristic. As

can be seen from Figure 13, this issue is obviously seen at hours 3, 11, 12, and 19 for the planning day.

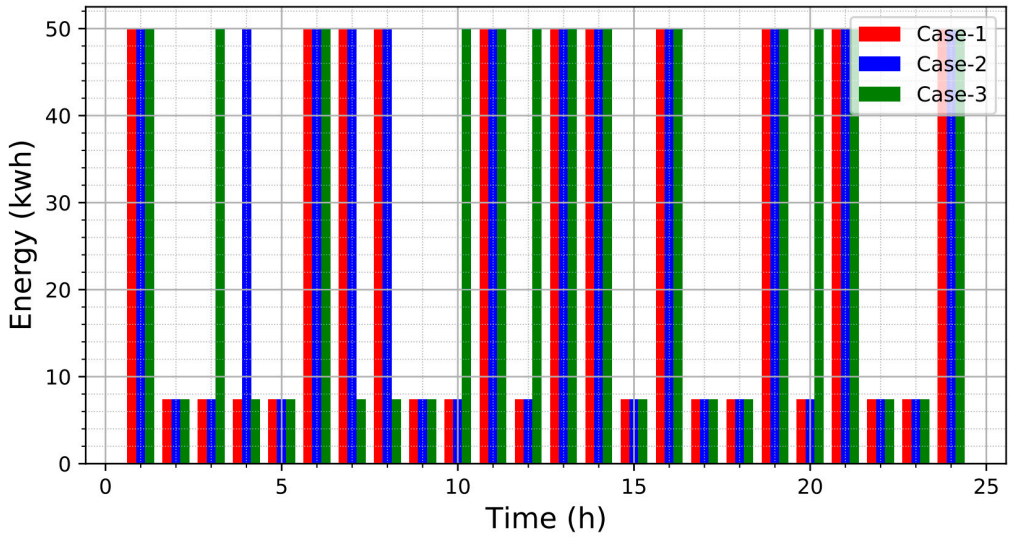

Figure 13. Hydrogen energy stored in HESS.

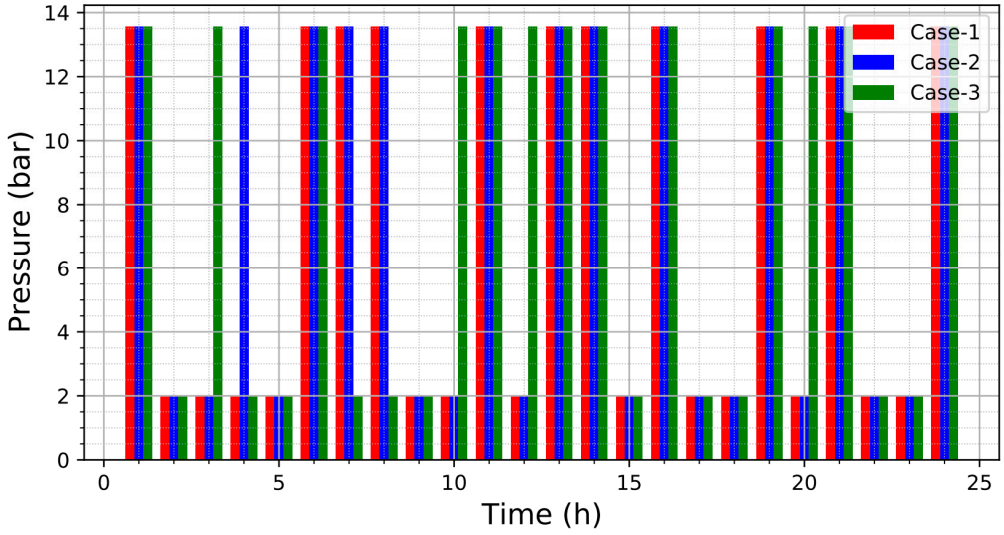

Figure 14. HESS pressure during different hours of planning period.

The results belonging to electrolyzer and fuel cell input power are indicated in Figures 15 and 16. From the economic point of view and according to the relatively low efficiency of the electrolyzer, this facility should be operated when the electrical price is significantly lower than the hydrogen price. Nevertheless, the main purpose of using electrolyzers and fuel cells is to reduce the emission of pollutants. As shown in Figure 15, the electrolyzer is mostly used in Case-1, because supplying its input power by the electrical grid will have a negative effect on the emission cost. At hours 1, 2, 7, and 8, the electrolyzer is employed to produce hydrogen from excess PV and WT electricity generation. Moreover, the electrolyzer is used during hours 15–18 only for Case-1, when electricity price is low and hydrogen price is high.

Figure 16 illustrates the fuel cell operates exactly opposite the electrolyzer. Since the fuel cell uses clean energy to produce electrical power, it is mostly used in Case-3. During hours 8–18, because of the high price of hydrogen, the fuel cell never operates in Case-1 and Case-2. At hours 13–18, when the wind speed is low and the solar radiation decreases, the fuel cell converts hydrogen into electricity in Case-3 to meet the electrical demand and

avoid buying more electricity from the grid and subsequent to it, increasing the emission cost.

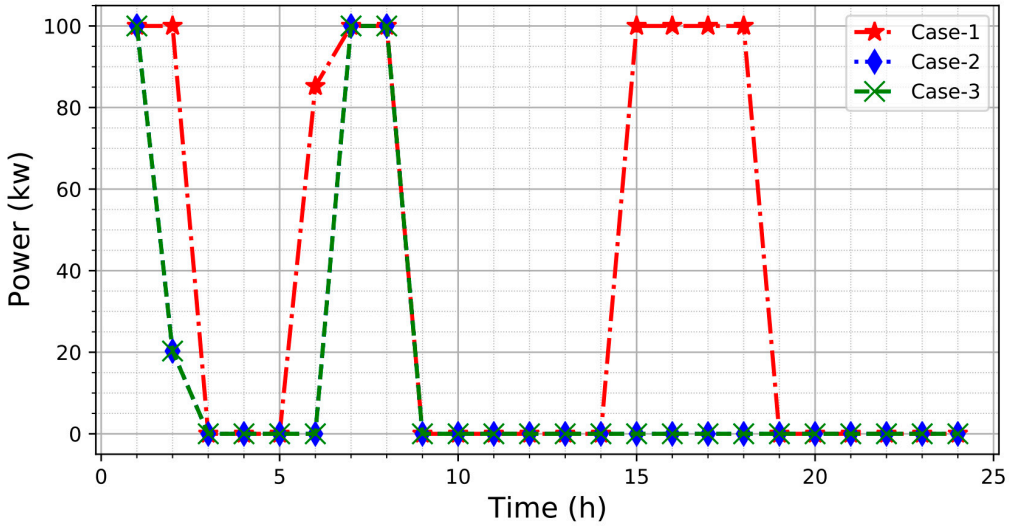

Figure 15. Electrolyzer input power during different hours of the planning day.

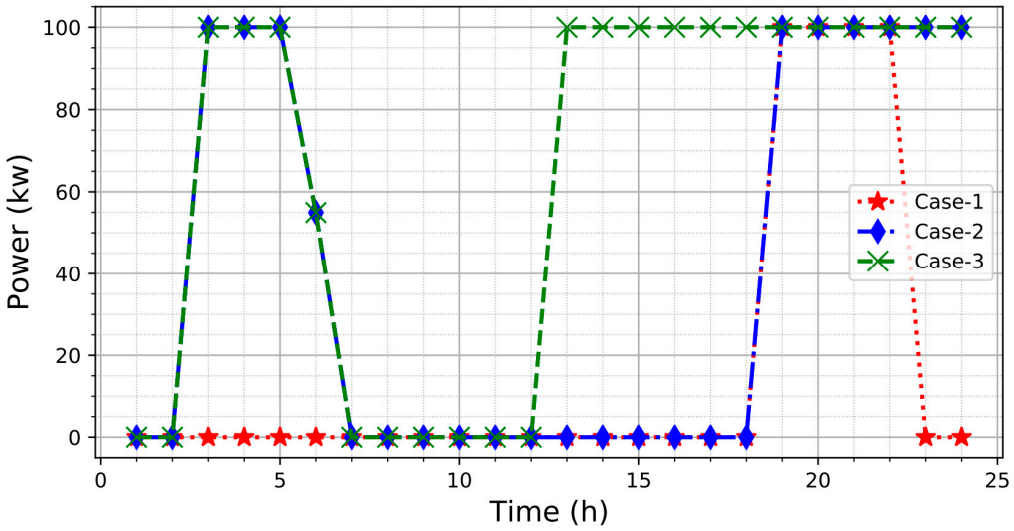

Figure 16. Fuel cell input power during different hours of the planning day.

Figure 17 shows the input power of boiler and CHP at each hour of the operation day. The boiler plays a key role in supplying the heat demand, so it produces its maximum power during most hours. At hours 9–10 and 14–16, the boiler meets all the heat demand without reaching its maximum power according to the heating load changes after applying DRP in the three cases, which are pictured in Figure 8. CHP is operated to generate electricity when the electrical grid inside the energy hub needs cheaper electricity. Furthermore, it could be also employed to produce heat when the boiler cannot supply all of the heat load. For the negative effect of CHP on emission cost, it is used less in Case-1 rather than in other cases. In summary, the participation of each energy hub's equipment, as well as energy networks, is presented in Table 4 and compared for different cases.

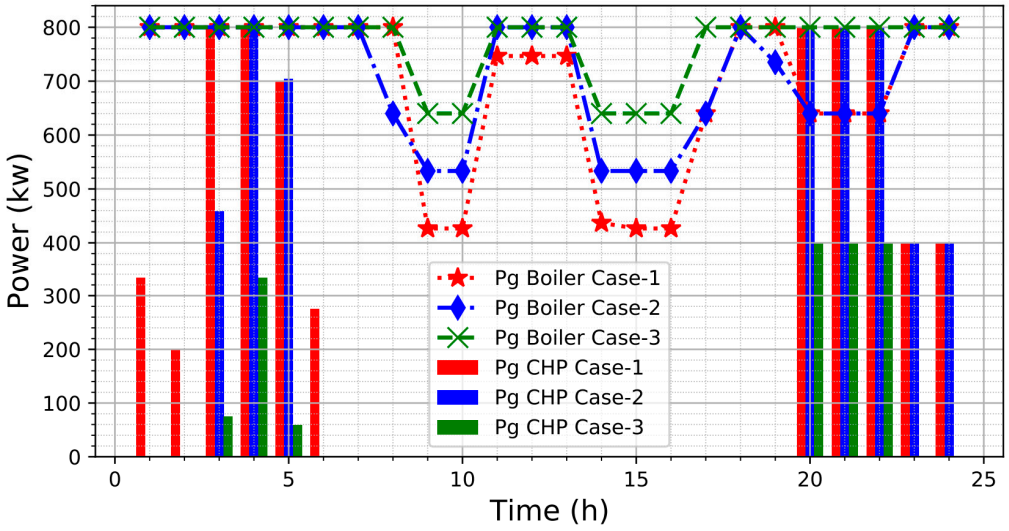

Figure 17. Input power of boiler and CHP.

Table 4. Participation rate of each network and facility in each case.

Facility/Network	Case-1	Case-2	Case-3
Electricity network	High	Normal	Low
Gas network	High	Normal	Low
Hydrogen network	Low	Normal	High
Boiler	Low	Normal	High
CHP	High	Normal	Low
Electrolyzer	High	Normal	Low
Fuel cell	Low	Normal	High

6.3. Optimization Analysis

After implementing SAUGMECON method, Pareto optimal solutions are obtained. Figure 18 shows the Pareto front for the proposed problem. As discussed earlier, the next step in the optimization phase is to find the most preferred solution, based on the system operator preference by using the AHP method. As can be seen in Figure 18, five different solutions, points A–E, are highlighted. Each point has been selected as the optimal solution for a specific preference as follows:

- Point A: Considered coefficient $\omega_1 = 1$ and $\omega_2 = 0$ (only economic preference);
- Point E: Considered coefficient $\omega_1 = 0.8$ and $\omega_2 = 0.2$ (Case-1);
- Point D: Considered coefficient $\omega_1 = 0.5$ and $\omega_2 = 0.5$ (Case-2);
- Point C: Considered coefficient $\omega_1 = 0.2$ and $\omega_2 = 0.8$ (Case-3);
- Point B: Considered coefficient $\omega_1 = 0$ and $\omega_2 = 1$ (only emission preference).

The value of objective cost functions obtained after solving the proposed problem with and without DRP in each case are shown in Tables 5 and 6, respectively. By comparing the results of these two tables, it is understood that DRP can reduce the objective function in all three cases. Respectively, 33.28%, 33.85, and 26.28% decrement in operation cost as well as 7.90%, 5.58%, and 8.36% decrement in the amount of pollution emission were obtained for the first, second, and third scenarios, which can show that the DPR can satisfactorily support the decrement of both economic and environmental costs.

The comparison between the obtained results of different cases, regarding operation and emission costs, are done in Figures 19 and 20, respectively. According to Figure 19, the operation cost for Case-1 is less than other cases and Figure 20 shows the emission cost has been decreased from Case-1 to Case-3. These results indicate the impact of the objective function coefficients. In other words, if the system operator as a decision maker cares more

about the economic cost, Case-1 is suitable for this goal. In contrast, if the decision maker prioritizes the emission cost, Case-3 would be more suitable than Case-1 and Case-2.

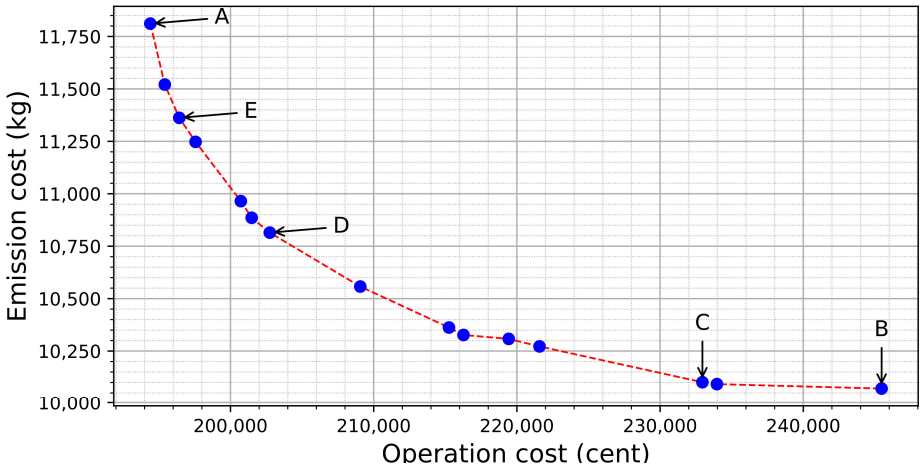

Figure 18. Pareto optimal solutions scatter.

Table 5. The objective functions cost with DRP.

Case#	ω_1	ω_2	Operation Cost (Cent)	Emission (kg)	Z
1	0.8	0.2	196,949.607	11,332.592	0.990
2	0.5	0.5	202,746.603	10,803.797	1.029
3	0.2	0.8	230,560.372	10,058.488	1.024

Table 6. The objective functions cost without DRP.

Case#	ω_1	ω_2	Operation Cost (Cent)	Emission (kg)	Z
1	0.8	0.2	262,495.055	12,228.062	1.07
2	0.5	0.5	271,369.829	11,406.413	1.113
3	0.2	0.8	291,144.340	10,898.993	1.093

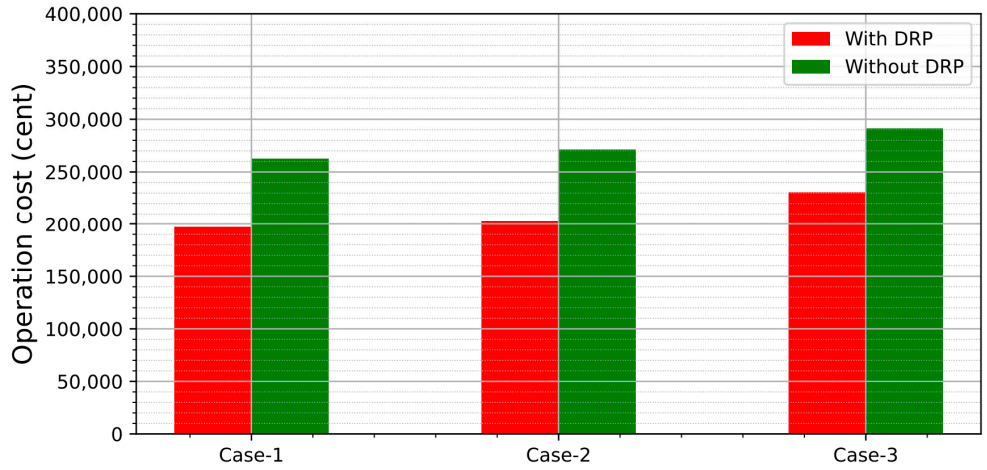

Figure 19. Operation cost comparison in three cases.

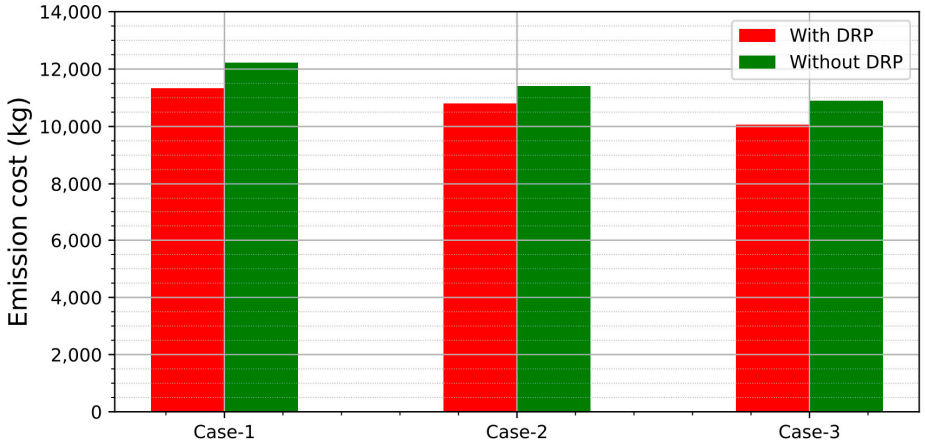

Figure 20. Emission cost comparison in three cases.

7. Conclusions

A novel scenario-based stochastic programming for the day-ahead operation problem of a hydrogen-based energy hub has been presented in this paper based on the multi-attribute decision-making approach. Moreover, a detailed model of the energy hub has been given and the performance of different hub facilities has been investigated. In this way, three different case studies have been applied, considering the various priorities for the weights of the objective functions. A pervasive analysis has been done on the hydrogen network and the results have shown the fuel cell plays an essential role in the proposed energy hub due to its free pollution characteristic, especially in Case-3. However, due to the high cost of electricity compared to hydrogen as well as the low efficiency of the electrolyzer, this equipment is rarely used. Moreover, both electrical and hydrogen energy storage systems have a more important role in Case-1 due to the economic preference of this case. By using the EDRP and TDRP, the total objective function of the proposed problem has been reduced by 8.08%, 8.163%, and 6.738% in Case-1, Case-2, and Case-3, respectively. Since in this study the focus was on the operation of the proposed energy hub and its optimal day-ahead scheduling, the planning and designing problem regarding the optimal placement and sizing of the different energy technologies would be considered in our future work.

Author Contributions: Conceptualization, M.L.I. and M.A.L.; methodology, M.L.I. and M.A.L.; software, M.L.I.; validation, M.L.I. and M.A.L.; formal analysis, M.L.I. and M.A.L.; investigation, M.L.I.; resources, M.L.I. and M.A.L.; data curation, M.L.I.; writing—original draft preparation, M.L.I.; writing—review and editing, M.A.L., M.S.G. and Z.Y.; visualization, M.L.I. and M.A.L.; supervision, M.S.G. and Z.Y.; project administration, M.A.L. and Z.Y.; funding acquisition, Z.Y. All authors have read and agreed to the published version of the manuscript.

Funding: This research is partially supported via AAU Bubble Project—A Novel Zero/Negative Emission Energy System Integrating Power-to-X, Allam Cycle, Carbon Capture, Utilization and Storage (CCUS) and CO2-based Energy Storage (AAU Project No. 762985).

Data Availability Statement: Data available on request due to restrictions e.g., privacy or ethical. The data presented in this study are available on request from the corresponding author. The data are not publicly available.

Conflicts of Interest: The authors declare no conflict of interest.

Nomenclature

Acronyms

P2H	Power to hydrogen
P2M	Power to methane
P2HH	Power-to-hydrogen and heat

SAUGMECON	Simple augmented e-constrained
MINLP	Mixed-integer non-linear programming
DRP	Demand response programming
TDRP	Thermal demand response programming
EDRP	Electrical demand response programming
IDRP	Integrated demand response programming
TOU	Time of use
RES	Renewable energy resource
PV	Photovoltaic
WT	Wind turbine
IGDT	Information gap decision theory
CHP	Combined heat & power
CCHP	Combined cooling, heat and power
ESS	Energy storage system
EESS	Electrical energy storage system
HESS	Hydrogen energy storage system
CM	Cost minimization
EM	Emission minimization
MOO	Multi-objective optimization
MOP	Multi-objective problem
DM	Decision making
AHP	Analytic hierarchy process
GAMS	General algebraic modeling system
Indices	
t	Time index
cr	Electricity and natural gas
n	Number of criteria
Parameters	
$\lambda_e, \lambda_g, \lambda_{H_2}$	Electricity, gas and hydrogen price
$\lambda_e^{ST}, \lambda_{H_2}^{ST}$	Electrical and hydrogen storages operation cost
λ_{cr}^{DR}	Electrical/Thermal DR operation cost
DR_{cr}	Rate of load reduction in electrical/thermal DRP
$Load$	Load after DRP
L_{inc}	Increased load in DRP
DR^{max}	Maximum rate of load reduction
γ_{CHP}, γ_B	CO2 emission factor of CHP and boiler
γ_e, γ_g	CO2 emission factor of electricity and gas network
D_e, D_h, D_{H_2}	Electrical, heat and hydrogen demand
η^T, η^C	Transformer and converter efficiencies
$\eta_e^{CHP}, \eta_h^{CHP}$	Gas to electricity and heat efficiency for CHP
η^B	Boiler efficiency
η^{EL}, η^{FC}	Electrolyzer and fuel cell efficiency
$P_{e\ storage}(initial)$	Initial amount of EESS
$P_{e\ storage}^{min}, P_{e\ storage}^{max}$	Minimum and maximum allowable amount of EESS
$P_{H_2\ storage}(initial)$	Initial amount of HESS
$P_{H_2\ storage}^{min}, P_{H_2\ storage}^{max}$	Minimum and maximum allowable amount of HESS
$P_{FC}^{min}, P_{FC}^{max}$	Minimum and maximum allowable amount of fuel cell
$P_{EL}^{min}, P_{EL}^{max}$	Minimum and maximum allowable amount of electrolyzer
P_e^{min}, P_e^{max}	Minimum and maximum allowable amount of purchased power from electrical network
P_g^{min}, P_g^{max}	Minimum and maximum allowable amount of purchased power from gas network
$P_{H_2}^{min}, P_{H_2}^{max}$	Minimum and maximum allowable amount of purchased power from hydrogen network
$P_g^{CHP\ max}, P_g^{B\ max}$	Maximum allowable amount of CHP and boiler power purchased from gas network
LHV_{H_2}	Lower heating value of the hydrogen
$\Re$	Gas constant

V_{H_2}	HESS volume
T_{H_2}	Inside temperature of the vessel
$Pr_{H_2}(initial)$	Initial amount HESS pressure
$Pr_{H_2}^{min}$, $Pr_{H_2}^{max}$	Minimum and maximum allowable amount HESS pressure
P_r	Wind turbine rated power
v	Wind speed
v_{co}, v_{ci}, v_r	Cut out, cut in and rated wind speed
Irr	Sun irradiation
Irr_0	Sun irradiation at the standard condition
P_{max}^M	Maximum electrical power generated at the standard condition
T	Ambiance temperature during a day
T_0	Module temperature at the standard condition
$NOCT$	Normal operation cell temperature of PV panel
RI	Relevant random index
Variables	
P_e	Amount of purchased electricity from electrical network
P_g	Amount of purchased natural gas from gas network
P_{H_2}	Amount of purchased hydrogen from hydrogen network
P_g^{CHP}	Amount of natural gas entering to the CHP
P_g^B	Amount of natural gas entering to the boiler
P_{wT}	Electrical power generated by WT
P_{PV}	Electrical power generated by PV
P_{EL}	Electrical power used by electrolyzer
P_{FC}	Electrical power used by fuel cell
$P_{H_2}^{ch}$	HESS charge power
$P_{H_2}^{dis}$	HESS discharge power
N_{EL}	Molar flow of electrolyzer
N_{FC}	Molar flow of fuel cell
Pr_{H_2}	HESS pressure
$Load$	Load after DRP
λ_{max}	Largest eigenvalue
RI	Relevant random index
Binary variables	
I_e	Decision variable for EESS
I_{H_2}	Decision variable for HESS
I_{FC}	Decision variable for fuel cell
I_{EL}	Decision variable for electrolyzer

References

1. Ali Lasemi, M.; Arabkoohsar, A.; Hajizadeh, A. Stochastic Multi-Objective Scheduling of a Wind Farm Integrated with High-Temperature Heat and Power Storage in Energy Market. *Int. J. Electr. Power Energy Syst.* **2021**, *132*, 107194. [CrossRef]
2. Kafaei, M.; Sedighizadeh, D.; Sedighizadeh, M.; Sheikhi, A. International Journal of Electrical Power and Energy Systems An IGDT / Scenario Based Stochastic Model for an Energy Hub Considering Hydrogen Energy and Electric Vehicles: A Case Study of Qeshm Island, Iran. *Int. J. Electr. Power Energy Syst.* **2022**, *135*, 107477. [CrossRef]
3. Lasemi, M.A.; Assili, M.; Hajizadeh, A. Smart Energy Management of Thermal Power Plants by Considering Liquid Fuel Dispatching System Modeling. In Proceedings of the 2018 Smart Grid Conference, SGC 2018, Sanandaj, Iran, 28–29 November 2018.
4. Ban, M.; Yu, J.; Shahidehpour, M.; Yao, Y. Integration of Power-to-Hydrogen in Day-Ahead Security-Constrained Unit Commitment with High Wind Penetration. *J. Mod. Power Syst. Clean Energy* **2017**, *5*, 337–349. [CrossRef]
5. Li, J.; Lin, J.; Song, Y.; Xing, X.; Fu, C. Operation Optimization of Power to Hydrogen and Heat (P2HH) in ADN Coordinated with the District Heating Network. *IEEE Trans. Sustain. Energy* **2019**, *10*, 1672–1683. [CrossRef]
6. Liu, J.; Sun, W.; Harrison, G.P. The Economic and Environmental Impact of Power to Hydrogen/Power to Methane Facilities on Hybrid Power-Natural Gas Energy Systems. *Int. J. Hydrogen Energy* **2020**, *45*, 20200–20209. [CrossRef]
7. Jahangir, M.H.; Javanshir, F.; Kargarzadeh, A. ScienceDirect Economic Analysis and Optimal Design of Hydrogen / Diesel Backup System to Improve Energy Hubs Providing the Demands of Sport Complexes. *Int. J. Hydrogen Energy* **2020**, *46*, 14109–14129. [CrossRef]

8. Shabani, M.J.; Moghaddas-Tafreshi, S.M. Fully-Decentralized Coordination for Simultaneous Hydrogen, Power, and Heat Interaction in a Multi-Carrier-Energy System Considering Private Ownership. *Electr. Power Syst. Res.* **2020**, *180*, 106099. [CrossRef]
9. Majidi, M.; Zare, K. Integration of Smart Energy Hubs in Distribution Networks under Uncertainties and Demand Response Concept. *IEEE Trans. Power Syst.* **2019**, *34*, 566–574. [CrossRef]
10. Jamalzadeh, F.; Hajiseyed Mirzahosseini, A.; Faghihi, F.; Panahi, M. Optimal Operation of Energy Hub System Using Hybrid Stochastic-Interval Optimization Approach. *Sustain. Cities Soc.* **2020**, *54*, 101998. [CrossRef]
11. Mansour-Saatloo, A.; Agabalaye-Rahvar, M.; Mirzaei, M.A.; Mohammadi-Ivatloo, B.; Abapour, M.; Zare, K. Robust Scheduling of Hydrogen Based Smart Micro Energy Hub with Integrated Demand Response. *J. Clean. Prod.* **2020**, *267*, 122041. [CrossRef]
12. Vehviläinen, I. Joint Assessment of Generation Adequacy with Intermittent Renewables and Hydro Storage: A Case Study in Finland. *Electr. Power Syst. Res.* **2021**, *199*, 107385. [CrossRef]
13. Daneshvar, M.; Mohammadi-Ivatloo, B.; Asadi, S.; Zare, K.; Anvari-Moghaddam, A. Optimal Day-Ahead Scheduling of the Renewable Based Energy Hubs Considering Demand Side Energy Management. In Proceedings of the 2019 International Conference on Smart Energy Systems and Technologies (SEST), Porto, Portugal, 9–11 September 2019; pp. 1–6. [CrossRef]
14. Turi, J.A.; Szyrocka, J.R.; Mansoor, M.; Asif, H.; Nazir, A.; Lorente, D.B. Assessing Wind Energy Projects Potential in Pakistan: Challenges and Way Forward. *Energies* **2022**, *15*, 9014. [CrossRef]
15. Javadi, M.S.; Lotfi, M.; Nezhad, A.E.; Anvari-Moghaddam, A.; Guerrero, J.M.; Catalao, J.P.S. Optimal Operation of Energy Hubs Considering Uncertainties and Different Time Resolutions. *IEEE Trans. Ind. Appl.* **2020**, *56*, 5543–5552. [CrossRef]
16. Bostan, A.; Nazar, M.S.; Shafie-khah, M.; Catalão, J.P.S. Optimal Scheduling of Distribution Systems Considering Multiple Downward Energy Hubs and Demand Response Programs. *Energy* **2020**, *190*, 116349. [CrossRef]
17. Karkhaneh, J.; Allahvirdizadeh, Y.; Shayanfar, H.; Galvani, S. Risk-Constrained Probabilistic Optimal Scheduling of FCPP-CHP Based Energy Hub Considering Demand-Side Resources. *Int. J. Hydrogen Energy* **2020**, *45*, 16751–16772. [CrossRef]
18. Oskouei, M.Z.; Member, S.; Mohammadi-ivatloo, B.; Member, S. Strategic Operation of a Virtual Energy Hub with the Provision of Advanced Ancillary Services in Industrial Parks. *IEEE Trans. Sustain. Energy* **2021**, *3029*, 2062–2073. [CrossRef]
19. Tao, Y.; Qiu, J.; Lai, S.; Zhao, J. Integrated Electricity and Hydrogen Energy Sharing in Coupled Energy Systems. *IEEE Trans. Smart Grid* **2021**, *12*, 1149–1162. [CrossRef]
20. AlRafea, K.; Fowler, M.; Elkamel, A.; Hajimiragha, A. Integration of Renewable Energy Sources into Combined Cycle Power Plants through Electrolysis Generated Hydrogen in a New Designed Energy Hub. *Int. J. Hydrogen Energy* **2016**, *41*, 16718–16728. [CrossRef]
21. Pan, G.; Gu, W.; Lu, Y.; Qiu, H.; Lu, S.; Yao, S. Optimal Planning for Electricity-Hydrogen Integrated Energy System Considering Power to Hydrogen and Heat and Seasonal Storage. *IEEE Trans. Sustain. Energy* **2020**, *11*, 2662–2676. [CrossRef]
22. Mansour-Satloo, A.; Agabalaye-Rahvar, M.; Mirazaei, M.A.; Mohammadi-Ivatloo, B.; Zare, K.; Anvari-Moghaddam, A. A Hybrid Robust-Stochastic Approach for Optimal Scheduling of Interconnected Hydrogen-Based Energy Hubs. *IET Smart Grid* **2021**, *4*, 241–254. [CrossRef]
23. Ranjbarzadeh, H.; Tafreshi, S.M.M.; Ali, M.H.; Kouzani, A.Z.; Khoo, S. A Probabilistic Model for Minimization of Solar Energy Operation Costs as Well as CO2 Emissions in a Multi-Carrier Microgrid (MCMG). *Energies* **2022**, *15*, 3088. [CrossRef]
24. Varasteh, F.; Nazar, M.S.; Heidari, A.; Shafie-khah, M.; Catalão, J.P.S. Distributed Energy Resource and Network Expansion Planning of a CCHP Based Active Microgrid Considering Demand Response Programs. *Energy* **2019**, *172*, 79–105. [CrossRef]
25. Kholardi, F.; Assili, M.; Lasemi, M.A.; Hajizadeh, A. Optimal Management of Energy Hub with Considering Hydrogen Network. In Proceedings of the 2018 International Conference on Smart Energy Systems and Technologies, SEST 2018, Sevilla, Spain, 10–12 September 2018; pp. 5–10.
26. Mokaramian, E.; Shayeghi, H.; Sedaghati, F.; Safari, A. Four-Objective Optimal Scheduling of Energy Hub Using a Novel Energy Storage, Considering Reliability and Risk Indices. *J. Energy Storage* **2021**, *40*, 102731. [CrossRef]
27. El-afifi, M.I.; Saadawi, M.M. Cogeneration Systems Performance Analysis as a Sustainable Clean Energy and Water Source Based on Energy Hubs Using the Archimedes Optimization Algorithm. *Sustainability* **2022**, *14*, 14766. [CrossRef]
28. Cau, G.; Cocco, D.; Petrollese, M.; Knudsen Kær, S.; Milan, C. Energy Management Strategy Based on Short-Term Generation Scheduling for a Renewable Microgrid Using a Hydrogen Storage System. *Energy Convers. Manag.* **2014**, *87*, 820–831. [CrossRef]
29. Najafi, A.; Pashaei, A.; Nojavan, S.; Majidi, M.; Hatami, H. A Stochastic Self-Scheduling Program for Compressed Air Energy Storage (CAES) of Renewable Energy Sources (RESs) Based on a Demand Response Mechanism. *Energy Convers. Manag.* **2016**, *120*, 388–396. [CrossRef]
30. Fahim, S.R.; Hasanien, H.M.; Turky, R.A.; Aleem, S.H.E.A.; Ćalasan, M. A Comprehensive Review of Photovoltaic Modules Models and Algorithms Used in Parameter Extraction. *Energies* **2022**, *15*, 8941. [CrossRef]
31. Zhang, W.; Reimann, M. A Simple Augmented ∈-Constraint Method for Multi-Objective Mathematical Integer Programming Problems. *Eur. J. Oper. Res.* **2014**, *234*, 15–24. [CrossRef]
32. Chen, W.H. Quantitative Decision-Making Model for Distribution System Restoration. *IEEE Trans. Power Syst.* **2010**, *25*, 313–321. [CrossRef]
33. Hemmati, M.; Abapour, M.; Mohammadi-Ivatloo, B.; Anvari-Moghaddam, A. Optimal Operation of Integrated Electrical and Natural Gas Networks with a Focus on Distributed Energy Hub Systems. *Sustainability* **2020**, *12*, 8320. [CrossRef]

34. Nojavan, S.; Zare, K.; Mohammadi-Ivatloo, B. Application of Fuel Cell and Electrolyzer as Hydrogen Energy Storage System in Energy Management of Electricity Energy Retailer in the Presence of the Renewable Energy Sources and Plug-in Electric Vehicles. *Energy Convers. Manag.* **2017**, *136*, 404–417. [CrossRef]
35. Amjady, N.; Aghaei, J.; Shayanfar, H.A. Stochastic Multiobjective Market Clearing of Joint Energy and Reserves Auctions Ensuring Power System Security. *IEEE Trans. Power Syst.* **2009**, *24*, 1841–1854. [CrossRef]